Computer Assisted Methods in Engineering and Science, **21**: 15–26, 2014.

Sequential stochastic identification of elastic constants using Lamb waves and particle filters

Marek Słoński
Cracow University of Technology, Institute for Computational Civil Engineering
Warszawska 24, 31-155 Kraków, Poland
e-mail: mslonski@L5.pk.edu.pl

Sequential stochastic identification of elastic parameters of thin aluminum plates using Lamb waves is proposed. The identification process is formulated as a Bayesian state estimation problem in which the elastic constants are the unknown state variables. The comparison of a sequence of numerical and pseudo-experimental fundamental dispersion curves is used for an inverse analysis based on particle filter to obtain sequentially the elastic constants. The proposed identification procedure is illustrated by numerical experiments in which the elastic parameters of an aluminum thin plate are estimated. The results show that the proposed approach is able to identify the unknown elastic constants sequentially and that this approach can be also useful for the quantification of uncertainty with respect to the identified parameters.

Keywords: Bayesian state estimation, particle filter, guided Lamb waves, dispersion curves, thin plate.

1. Introduction

Lamb waves have been used for three decades for non-destructive identification of elastic constants of plate structures. The reconstruction can be based on the minimization of the sum of the squares of the discrepancy between experimental and analytical or numerical dispersion curves. Rogers in [5] demonstrated identification of elastic properties with several materials (aluminum, steel, glass) and with both thick (6 mm) and thin plates (0.8 mm) using nonlinear least squares. He also investigated the sensitivity of the nonlinear least squares solution to the measurement region of the dispersion curve and he found that identification is more accurate when only selected frequencies are used.

Recently, Sale et al. in [8] proposed reconstruction of elastic moduli of plate-like structures based on fundamental symmetric and antisymmetric dispersion curves obtained through a semi-analytical finite element (SAFE) formulation and corresponding numerical or experimental curves. The SAFE method coupled to the inverse procedure was tested by identification of the elastic material properties of a 2.54 mm thick aluminum plate. It was found that by applying both fundamental symmetric and antisymmetric dispersion curves smaller residual error was obtained.

Up to date, most of the Lamb wave-based identification methods for elastic constants of plates can be categorized as deterministic approaches. They provide only numerical values for the elastic properties and often fail to fully characterize reconstruction uncertainty in systematic manner. In this context Bayesian methods offer more systematic approach to uncertainty quantification. For example, Gogu et al. in [3] adopted Bayesian framework for identifying elastic constants of an orthotropic composite plate from an open-hole tensile test with full-field displacement measurements. They found that Bayesian approach is a worthwhile undertaking since it allows more accurate representation of experimental uncertainty as well a solid basis for combining measurements and their uncertainties stemming from different sources.

Bayesian approach is also sequential in nature allowing for solving identification problems recursively at every acquisition of measurements. Furukawa and Pan in [2] proposed an energy-based

characterization technique that recursively identifies the elastic constants of anisotropic materials using Kalman filter. They compared the proposed technique with a deterministic technique based on solving a set of linear equations and have shown that the filtering-based technique is not only more robust to measurement noise but also describes uncertainty in the identified constants. Recently, Tekieli and Słoński in [9] compared Kalman filter and Monte Carlo filter (a.k.a. particle filter) in the problem of Young's modulus identification of a laboratory-scale frame. They have shown that Monte Carlo filter can be a viable alternative to Kalman filter, especially in case of nonlinear problems.

In this paper, a novel application of particle filter for sequential stochastic identification of elastic constants of plate structures using Lamb waves is proposed. The proposed procedure is based on the comparison of experimental and analytical or numerical dispersion curves and the identification results are in the form of a posterior distribution over elastic constants which describe the uncertainty. The proposed procedure is verified on an example of pseudo-experimental dispersion curves computed for an aluminum plate.

The paper is organized as follows. Section 2 briefly describes the semi-analytical procedure for computing the dispersion curves based on Rayleigh-Lamb equations. A short presentation of particle filter-based sequential stochastic identification technique in the context of Bayesian state estimation is given in Sec. 3. Section 4 contains a numerical study for verification of the proposed approach. Closing remarks are presented in Sec. 5.

2. Lamb waves for elastic plates

2.1. Rayleigh-Lamb equations

Nondestructive identification of elastic constants of thin plates can be based on dispersion curves derived for guided ultrasonic waves propagating in elastic plates. In case of a homogeneous isotropic and elastic infinite plate, the propagation of ultrasonic waves, assuming plane strain, is described by Lamb waves theory [4, 6]. The waves propagating in these plates are dispersive and have infinite number of symmetric and anti-symmetric modes that are characterized by dispersion curves.

The dispersion curves are usually computed by numerical solution of Rayleigh-Lamb characteristic equations. In case of symmetric waves, the dispersion curves are computed from the following equation

$$\frac{\tan(\beta h)}{\tan(\alpha h)} = -\frac{4\alpha\beta k^2}{(k^2-\beta^2)^2}, \tag{1}$$

where $\alpha^2 = \dfrac{\omega^2}{c_L^2} - k^2$ and $\beta^2 = \dfrac{\omega^2}{c_T^2} - k^2$. ω is the frequency, k is the wavenumber, plate thickness is $d = 2h$, c_L, c_T are wave velocities and ν is the Poisson's ratio. The velocities of respectively transverse waves c_L and longitudinal waves c_T are given by

$$c_L = \sqrt{\frac{\lambda+2\mu}{\rho}} = \sqrt{\frac{E}{\rho}\frac{1-\nu}{(1+\nu)(1-2\nu)}}, \qquad c_T = \sqrt{\frac{\mu}{\rho}} = \sqrt{\frac{E}{\rho}\frac{1}{2(1+\nu)}}, \tag{2}$$

where μ is the first Lamé constant, λ is the second Lamé constant and ρ is the mass density. From Eq. (2), we can see that the ratio of velocities $\kappa = \dfrac{c_L}{c_T}$ depends only on the Poisson's ratio as

$$\kappa = \frac{2(1-\nu)}{1-2\nu} > \frac{4}{3}. \tag{3}$$

In case of antisymmetric waves, the dispersion curves are computed from a similar equation as

$$\frac{\tan(\beta h)}{\tan(\alpha h)} = -\frac{(k^2-\beta^2)^2}{4\alpha\beta k^2}. \tag{4}$$

A semi-analytical approach for efficient solution of Rayleigh-Lamb equations is based on the introduction of non-dimensional frequency and wavenumber variables in the form [1]

$$\Omega = \frac{\omega h}{c_T}, \qquad \xi = kh, \tag{5}$$

and the following two equations

$$x = (\Omega^2 - \xi^2)^{1/2}, \qquad y = (\Omega^2 \kappa^{-2} - \xi^2)^{1/2}. \tag{6}$$

Substituting the non-dimensional variables into the frequency Eqs. (1) and (4) we obtain

$$\frac{4xy\xi^2}{(\xi^2 - x^2)^2} + \frac{\tan(x)}{\tan(y)} = 0, \qquad \text{for symmetric waves,} \tag{7}$$

$$\frac{4xy\xi^2}{(\xi^2 - x^2)^2} + \frac{\tan(y)}{\tan(x)} = 0, \qquad \text{for antisymmetric waves.} \tag{8}$$

After some additional transformations, the Rayleigh-Lamb equations for plates in non-dimensional variables have the form

$$(\xi^2 - x^2)^2 \sin(x)\cos(y) + 4xy\xi^2 \cos(x)\sin(y) = 0, \qquad \text{for symmetric modes,} \tag{9}$$

$$(\xi^2 - x^2)^2 \sin(y)\cos(x) + 4xy\xi^2 \cos(y)\sin(x) = 0, \qquad \text{for antisymmetric modes.} \tag{10}$$

These equations are solved numerically for the roots which form the basis for obtaining non-dimensional dispersion curves. Figure 1 shows two fundamental non-dimensional dispersion curves S_0 and A_0, which were computed using Eqs. (9) and (10) assuming Poisson's ratio $\nu = 0.33$.

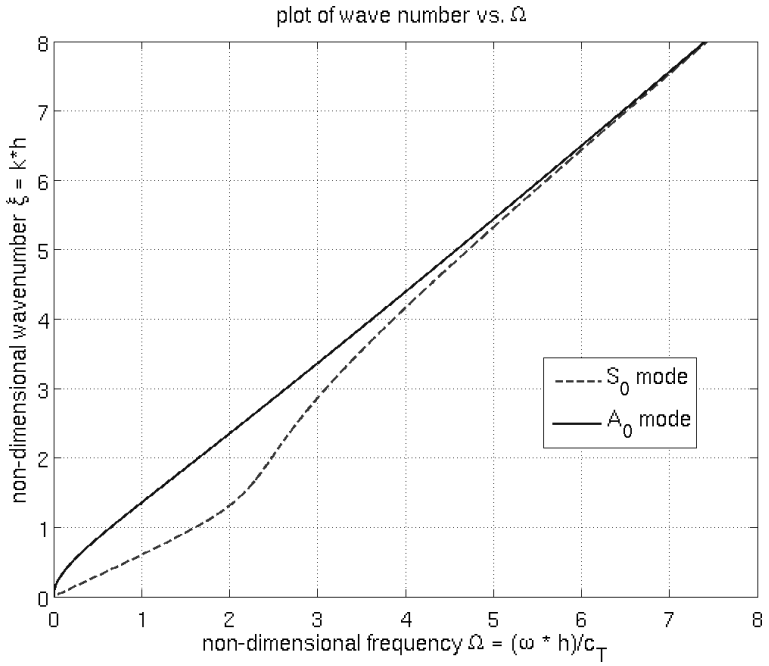

Fig. 1. Plot of fundamental non-dimensional dispersion curves S_0 and A_0 computed using Eqs. (9) and (10) for $\nu = 0.33$.

2.2. Dispersion curves

From the non-dimensional relation between Ω and ξ, using equations in (5), we can compute the fundamental dispersion curves for specified values of Young's modulus E, half of the plate thickness d and the mass density ρ. Each dispersion curve consists of points defined as a pair of frequency value and the corresponding wavenumber. For example, in Fig. 2, three dispersion curves are presented obtained assuming the plate thickness $d = 2$ mm, the mass density $\rho = 2700$ kg/m^3 and three values of Young's modulus E in range from 60 GPa to 70 GPa. It can be seen from this plot that the value of Young's modulus has rather small influence on the shape of the dispersion curves.

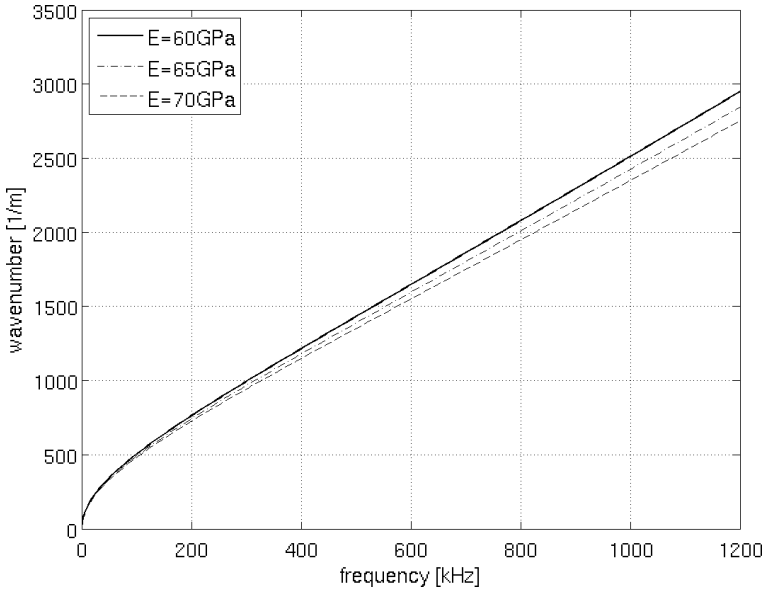

Fig. 2. Plot of fundamental dispersion curves A_0 computed for Poisson's ratio $\nu = 0.33$, half of plate thickness $d = 2$ mm, mass density $\rho = 2700$ kg/m^3 and three Young's moduli E.

3. Sequential stochastic identification

3.1. Bayesian state estimation

Sequential identification of elastic constants proposed in this paper is based on Bayesian inference for a nonlinear stationary dynamical system defined in the discrete state space form. The formulation of Bayesian state estimation problem for a dynamical system consists of two nonlinear equations. The first equation is called a transition model and is defined by

$$\mathbf{x}_{k+1} = \mathbf{f}(\mathbf{x}_k, \mathbf{w}_{k+1}), \qquad k = 1, ..., K, \tag{11}$$

where $\mathbf{x}_k$ denotes the set of state variables at time step k. The function $\mathbf{f}(\cdot)$ is a transition function and it defines the evolution of state variables. The system evolution process is corrupted by a random noise represented in Eq. (11) by a vector of random variables $\mathbf{w}_k$.

The second equation is called an observation model and is defined by

$$\mathbf{y}_{k+1} = \mathbf{h}(\mathbf{x}_{k+1}, \mathbf{v}_{k+1}), \qquad k = 1, ..., K, \tag{12}$$

$\mathbf{y}_k$ denotes the set of observable variables at time step k. The output from the dynamical system $\mathbf{y}_k$ is measured at each time k, and the measurements sequence up to time k is stored in the matrix $\mathbf{Y}_{1:k} = \{\mathbf{y}_1, \mathbf{y}_2, \ldots, \mathbf{y}_k\}$. The function $\mathbf{h}(\cdot)$ is an observation (measurement) function and it defines

the measurement process as a function of state variables. Similarly, the measurement process is also corrupted by a random noise represented in Eq. (12) by a vector of random variables $\mathbf{v}_k$.

Bayesian state estimation problem can be graphically presented in the form of a dynamic Bayesian network, see Fig. 3. Bayesian network is a directed acyclic graph and represents the dependencies among random variables [7]. In this context, Kalman filter is an example of dynamic Bayesian network with continuous variables and linear Gaussian conditional distributions. Dynamic Bayesian network can model any distribution in which the joint distribution over the sequence of K observed variables $\mathbf{y}_k$ and state (hidden) variables $\mathbf{x}_k$ is given by

$$p(\mathbf{x}_1, \mathbf{x}_2, \ldots, \mathbf{x}_K; \mathbf{y}_1, \mathbf{y}_2, \ldots, \mathbf{y}_K) = p(\mathbf{x}_1) \prod_{k=2}^{K} p(\mathbf{x}_k|\mathbf{x}_{k-1}) \prod_{k=1}^{K} p(\mathbf{y}_k|\mathbf{x}_k), \tag{13}$$

where $p(\mathbf{x}_k|\mathbf{x}_{k-1})$ is the transition model (assumed here to be a first-order Markov chain) and $p(\mathbf{y}_k|\mathbf{x}_k)$ is the observation (measurement) model.

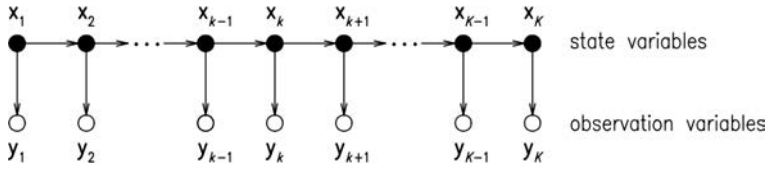

Fig. 3. Dynamic Bayesian network for a sequence of state variables $\mathbf{x}_k$ and observable variables $\mathbf{y}_k$ (measurements).

The main goal of Bayesian state estimation is sequential inference of the posterior distribution $p(\mathbf{x}_{k+1}|\mathbf{Y}_{1:k+1})$ starting from a prior distribution $p(\mathbf{x}_k|\mathbf{Y}_{1:k})$. The inference is performed recursively in two steps: prediction step and update (correction) step. In the first step the prediction of state variables distribution $p(\mathbf{x}_{k+1}|\mathbf{y}_k)$ before applying new measurements is done. This distribution is computed using the sum rule of probability and integrating out the state variables as

$$p(\mathbf{x}_{k+1}|\mathbf{Y}_{1:k}) = \int p(\mathbf{x}_{k+1}|\mathbf{x}_k) p(\mathbf{x}_k|\mathbf{Y}_{1:k}) d\mathbf{x}_k. \tag{14}$$

Then, the new measurements $\mathbf{y}_{k+1}$ are used to update the prior to obtain the posterior distribution $p(\mathbf{x}_{k+1}|\mathbf{Y}_{1:k+1})$ applying the Bayes' rule

$$p(\mathbf{x}_{k+1}|\mathbf{Y}_{1:k+1}) = \frac{p(\mathbf{y}_{k+1}|\mathbf{x}_{k+1}) p(\mathbf{x}_{k+1}|\mathbf{Y}_{1:k})}{p(\mathbf{y}_{k+1}|\mathbf{Y}_{1:k})}, \tag{15}$$

where the denominator in (15) is computed from

$$p(\mathbf{y}_{k+1}|\mathbf{Y}_{1:k}) = \int p(\mathbf{y}_{k+1}|\mathbf{x}_{k+1}) p(\mathbf{x}_{k+1}|\mathbf{Y}_{1:k}) d\mathbf{x}_{k+1}. \tag{16}$$

The update step in Eq. (15) can be also written in the recursive form that is more useful for obtaining particle filter algorithm. Using Bayes' rule we can rewrite Eq. (15) as

$$p(\mathbf{x}_{k+1}|\mathbf{Y}_{1:k+1}) = p(\mathbf{x}_k|\mathbf{Y}_{1:k}) \frac{p(\mathbf{y}_{k+1}|\mathbf{x}_{k+1}) p(\mathbf{x}_{k+1}|\mathbf{x}_k)}{p(\mathbf{y}_{k+1}|\mathbf{Y}_{1:k})}. \tag{17}$$

3.2. Particle filter

The Bayesian state estimation described above gives the posterior distribution over the states. It does not give, however, the way to find the solution efficiently using both Eqs. (14) and (15).

In addition, the exact inference is intractable and an approximate method has to be applied. In this work a particle filter (PF) algorithm is used. It is based on sequential Monte Carlo sampling and is described below.

In order to implement Bayesian filtering, we approximate the posterior distribution $p(\mathbf{x}_{k+1}|\mathbf{y}_{k+1})$ using N particles $\mathbf{x}^i_{k+1}, (i = 1, 2, \ldots, N)$, with corresponding importance weights w^i_{k+1}, that replace the posterior distribution with the empirical distribution

$$P_N(\mathbf{x}_{k+1}) = \sum_{i=1}^{N} w^i_{k+1}\delta(\mathbf{x}_{k+1} - \mathbf{x}^i_{k+1}), \tag{18}$$

where $\delta(\cdot)$ is the Dirac delta function. The weights are computed using sequential importance sampling as

$$w^i_{k+1} = w^i_k \frac{p(\mathbf{y}_{k+1}|\mathbf{x}^i_{k+1})p(\mathbf{x}^i_{k+1}|\mathbf{x}^i_k)}{\pi(\mathbf{x}^i_{k+1}|\mathbf{x}^i_k, \mathbf{y}_{k+1})}, \tag{19}$$

where $\pi(\mathbf{x}_{k+1}|\mathbf{x}_k, \mathbf{y}_{k+1})$ is the importance distribution such that samples from it can be easily generated. In general, choosing the optimal importance distribution is rather difficult so for simplicity, the common choice is to apply the transition density as the importance density

$$\pi(\mathbf{x}^i_{k+1}|\mathbf{x}^i_k, \mathbf{y}_{k+1}) = p(\mathbf{x}^i_{k+1}|\mathbf{x}^i_k), \tag{20}$$

that yields a simple equation for computing weights in the next time step as

$$w^i_{k+1} = w^i_k \; p(\mathbf{y}_{k+1}|\mathbf{x}^i_{k+1}). \tag{21}$$

Note that these weights are normalized and satisfy $0 \leq \; w^i_k \; \leq 1$ and $\sum\limits_{i=1}^{N} w^i_k = 1$.

The initial weights are uniform with values $w^i_1 = 1/N$ but later during recursive computations they become far from uniform leading to particles degradation (few particles with large weights). As a result the empirical distribution becomes very poor approximation of the state variables distribution $p(\mathbf{x}_{k+1}|\mathbf{Y}_{1:k+1})$. To overcome this particular degradation problem, a sequential resampling procedure is applied. The resampling procedure regenerates the set of particles by replicating the particles with high importance weights and removing samples with low weights.

Finally, the basic particle filter algorithm is as follows. It starts with a population of N initial-state samples, created by sampling from the prior $p(\mathbf{x}_1)$. Then the prediction-update-resample cycle is repeated for each time step [7]:

1. Each sample is propagated forward by sampling the next state value $\mathbf{x}_{k+1}$, given the current value $\mathbf{x}_k$ for the sample, based on the transition model $p(\mathbf{x}_{k+1}|\mathbf{x}_k)$.

2. Each sample is weighted by the likelihood it assigns to the new evidence, $p(\mathbf{y}_{k+1}|\mathbf{x}_{k+1})$.

3. The population is resampled to generate a new population of N samples. Each new sample is selected from the current population; the probability that a particular sample is selected is proportional to its weight. The new samples are unweighted.

3.3. Identification of elastic constants of plates

In the second section, we formulated the sequential stochastic identification problem as a Bayesian state estimation problem. Because the plate parameters are assumed to not change in time, they are treated here as time-independent state variables and the transition equation has the following simple form:

$$\mathbf{x}_{k+1} = \mathbf{x}_k. \tag{22}$$

The Eq. (22) is further modified as

$$\mathbf{x}_{k+1} = \mathbf{x}_k + \mathbf{w}_{k+1}, \tag{23}$$

where $\mathbf{w}_k$ is a noise random variables added for numerical efficiency of particle filter-based identification. In this work, $\mathbf{w}$ is assumed to be a set of independent and identically distributed (iid) Gaussian random variables

$$p(\mathbf{w}) = \mathcal{N}(\mathbf{w}|\mathbf{0}, \boldsymbol{\sigma}_w^2), \tag{24}$$

where $\boldsymbol{\sigma}_w^2$ is a covariance matrix.

The states are recursively estimated using measurements $\mathbf{y}_{k+1}$ that here are defined as the fundamental antisymmetric dispersion curves A_0. They are related to state variables $\mathbf{x}_{k+1}$ by the nonlinear observation model $\mathbf{h}(\mathbf{x}_{k+1}, \mathbf{v}_{k+1})$ as

$$\mathbf{y}_{k+1} = \mathbf{h}(\mathbf{x}_{k+1}) + \mathbf{v}_{k+1}, \tag{25}$$

where $\mathbf{v}_{k+1}$ is a noise random variables introduced to account for modeling and measurement uncertainties. Here it is also assumed to be a set of independent and identically distributed (iid) Gaussian random variables

$$p(\mathbf{v}) \propto \mathcal{N}(\mathbf{v}|\mathbf{0}, \boldsymbol{\sigma}_v^2), \tag{26}$$

where $\boldsymbol{\sigma}_v^2$ is a covariance function.

Finally, the proposed approach is graphically presented in Fig. 4 in the form of a flowchart.

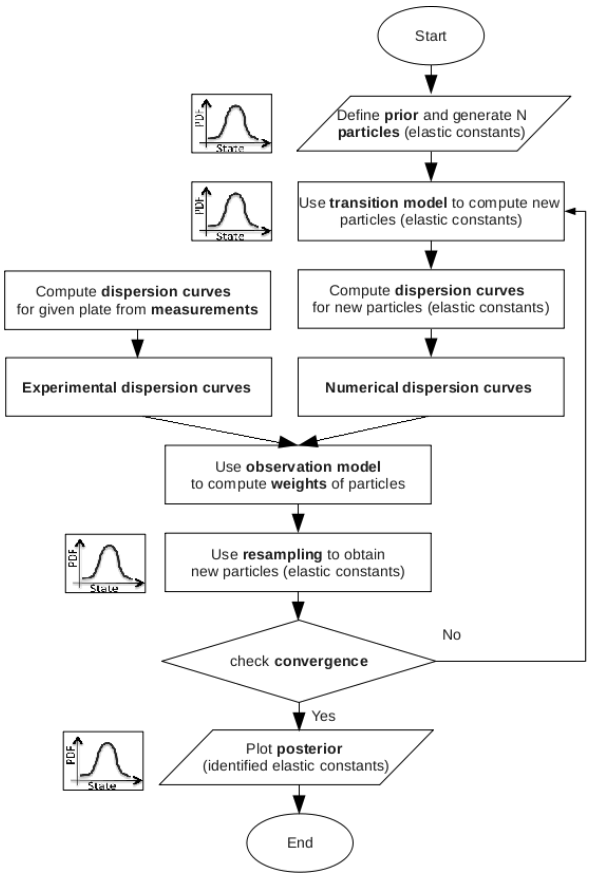

Fig. 4. Flowchart of particle filter-based identification of elastic constants of thin plates using experimental and numerical dispersion curves.

4. Numerical experiments

To assess the effectiveness of the proposed method, numerical exercises for an aluminum plate were performed. In the numerical experiments, the material properties of the aluminum plate (Young's modulus, Poisson's ratio and mass density) and the plate thickness were assumed in advance, see Table 1 for exact values of these parameters.

Table 1. Assumed values of the aluminum plate parameters applied in the numerical experiments.

Parameter	E [GPa]	ν [–]	ρ [kg/m^3]	h [mm]
Assumed value	67.5	0.33	2700	4

Having defined the plate parameters, a pseudo-experimental fundamental antisymmetric dispersion curve A_0 was computed using semi-analytical approach described above. During sequential identification, this curve was represented with a small number of parameters that were used as the observed variables $\mathbf{y}$.

4.1. Young's modulus identification

4.1.1. State-space model definition

One-dimensional transition model

In the first experiment, we assumed that the Young's modulus is a time-independent state variable and the transition equation for a state-space model is defined by (23). The state variable x_k is defined as the Young's modulus in k-th step $x_k = E_k$ and w_k denotes an independent and identically distributed (iid) Gaussian random variable with zero mean and variance σ_x^2, defined by (24). The value of σ_x was set to 0.003 GPa.

Observation equation

The vector of observed variables $\mathbf{y}_{k+1}$ was defined as a set of parameters of the fundamental antisymmetric dispersion curves A_0. The observed variables are related to the state variable x_{k+1} by the nonlinear observation function $\mathbf{h}(x_{k+1})$, defined in (25). The vector $\mathbf{v}_{k+1}$ denotes an independent and identically distributed (iid) multivariate Gaussian random variable with zero mean vector and covariance matrix $\boldsymbol{\sigma}_y^2$. The covariance matrix was defined as a diagonal isotropic matrix with elements σ_y equal to 0.01 1/m. Finally, the nonlinear observation function $\mathbf{h}(x_{k+1})$ was used to predict the parameters of the fundamental dispersion curve for a given Young's modulus.

Prior distribution

Our initial and uncertain knowledge about the state variable (here Young's modulus) is represented by a prior distribution $p(x_0)$. In the experiments, we applied a one-dimensional normal prior distribution $p(x_0) = \mathcal{N}(\mu_0, \sigma_0^2)$, with mean value $\mu_0 = 67.0$ GPa and standard deviation $\sigma_0 = 3.35$ GPa (coefficient of variation (COV) was 5%). Figure 5 shows the plot of the prior distribution (as a dashed line).

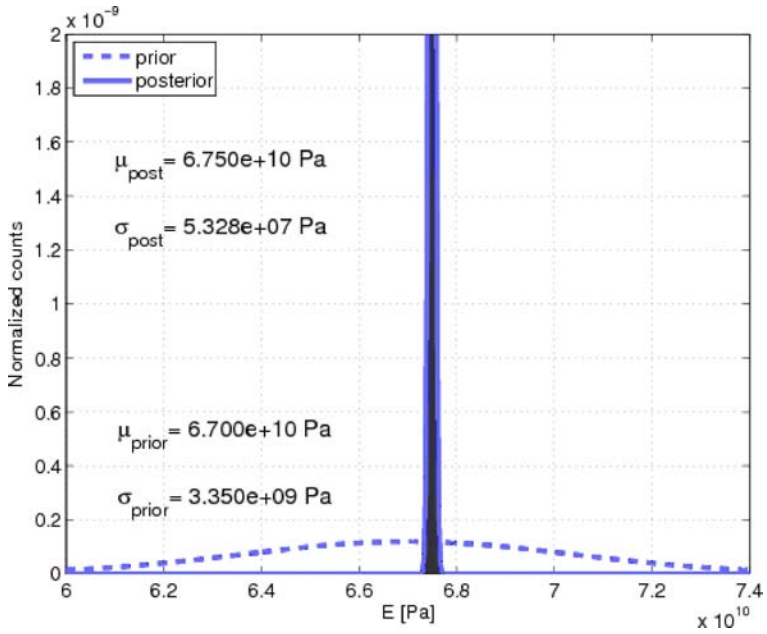

Fig. 5. Plot of prior and posterior distributions for Young's modulus. Gaussian prior distribution (dashed line) has mean value $\mu_{\text{prior}} = 67.0$ GPa and standard deviation $\sigma_{\text{prior}} = 3.35$ GPa (coefficient of variation (COV) is 5%). Approximate Gaussian posterior distribution (solid line) has mean value $\mu_{\text{pos}} = 67.5$ GPa and standard deviation $\sigma_{\text{pos}} = 0.05$ GPa (coefficient of variation (COV) is 0.1%).

4.1.2. Young's modulus identification results

The approximate posterior distribution of Young's modulus given pseudo-experimental dispersion curves $P_N(x_k|\mathbf{y}_k)$ in the k-th step was computed using the particle filter-based identification procedure described above. In experiments, we applied $N = 2000$ particles to obtain the approximate posterior distribution and the number of steps in the sequential identification was set to $K = 500$. Figure 6 shows the sequential nature of the elastic constant identification process by plotting the

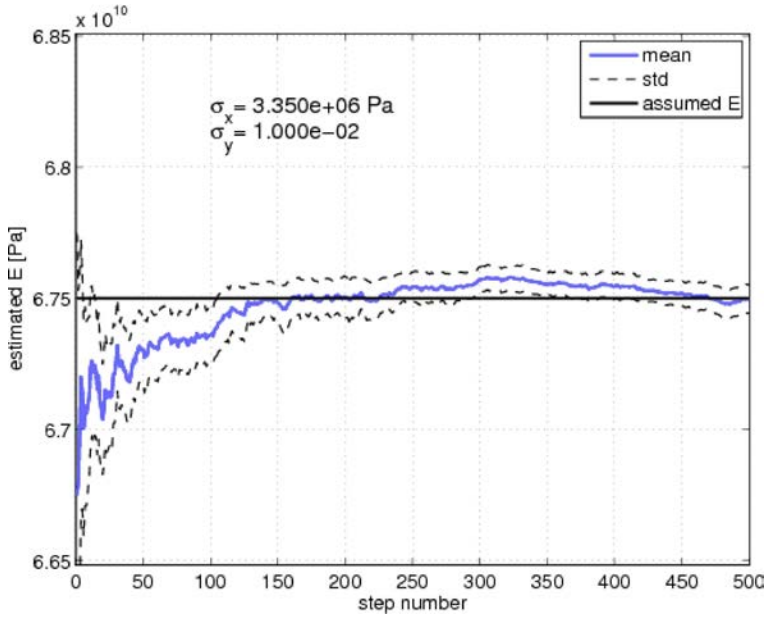

Fig. 6. Plot of evolution of mean value of posterior distribution for Young's modulus and corresponding one-standard deviation error bars (solid horizontal line represents Young's modulus value (67.5 GPa) assumed in numerical experiments).

evolution of the mean value of the posterior distribution and the corresponding plot for the one-standard deviation error bars as a function of the step number. There is also shown a solid horizontal line representing the reference Young's modulus value (67.5 GPa) applied in numerical experiments. From the plot, it may be observed that the estimation process converged to the reference value quite rapidly (in about 120 iterations).

Table 2 presents statistical parameters of prior and posterior distributions in the form of mean values, standard deviations and coefficients of variation (COV). From the table, it can be stated that the final mean value of the posterior distribution is the same as the reference value. Moreover, the coefficient of variation decreased from 5% for the prior distribution to only 0.1% for the final posterior distribution. Figure 5 shows the final one-dimensional posterior distribution together with the prior distribution.

Table 2. Statistical parameters of prior and posterior distributions for Young's modulus (mean value, standard deviation and coefficient of variation (COV)).

Parameter	Prior	Posterior
Mean value (GPa)	67.0	67.5
Standard deviation (GPa)	3.35	0.05
COV (%)	5.0	0.1

4.2. Identification of Young's modulus and Poisson's ratio

4.2.1. State-space model definition

Two-dimensional transition model

In this example, we assumed that Young's modulus and Poisson's ratio were time-independent state variables and the transition equation for a state-space model is defined by (23). The vector of the state variables $\mathbf{x}_k$ consists of the Young's modulus and Poisson's ratio in k-th step $\mathbf{x}_k = \{E_k, \nu_k\}$. The vector $\mathbf{w}_k$ denotes independent and identically distributed (iid) Gaussian random variables with zero mean vector and covariance matrix $\boldsymbol{\sigma}_w^2$, defined by (24). The covariance matrix was defined as a diagonal isotropic matrix with elements σ_x equal to 0.003 GPa and 0.0015, respectively.

Observation equation

In the experiments we used a vector of observed variables $\mathbf{y}_{k+1}$ which were defined as parameters of the fundamental antisymmetric dispersion curves A_0. The observed variables are related to the state variable x_{k+1} by the nonlinear observation function $\mathbf{h}(x_{k+1})$, defined in (25), where $\mathbf{v}_{k+1}$ denotes an independent and identically distributed (iid) multivariate Gaussian random variable with zero mean vector and covariance matrix $\boldsymbol{\sigma}_y^2$. The covariance matrix was defined as a diagonal isotropic matrix with elements σ_y equal to 0.01 1/m. The nonlinear observation function $\mathbf{h}(x_{k+1})$ was used to predict the parameters of the fundamental dispersion curve for a given Young's modulus and Poisson's ratio.

Prior distribution

The uncertainty about Young's modulus and Poisson's ratio values was represented by a two-dimensional Gaussian prior distribution $p(\mathbf{x}_0) = \mathcal{N}(\boldsymbol{\mu}_0, \boldsymbol{\sigma}_0^2)$, with mean values $\boldsymbol{\mu}_0 =$ [67.1 GPa, 0.33]. The standard deviations were about 5% of the corresponding mean values, i.e., $\boldsymbol{\sigma}_0 =$ [3.4 GPa, 0.02]. Figure 7 shows a contour plot of the two-dimensional prior together with the

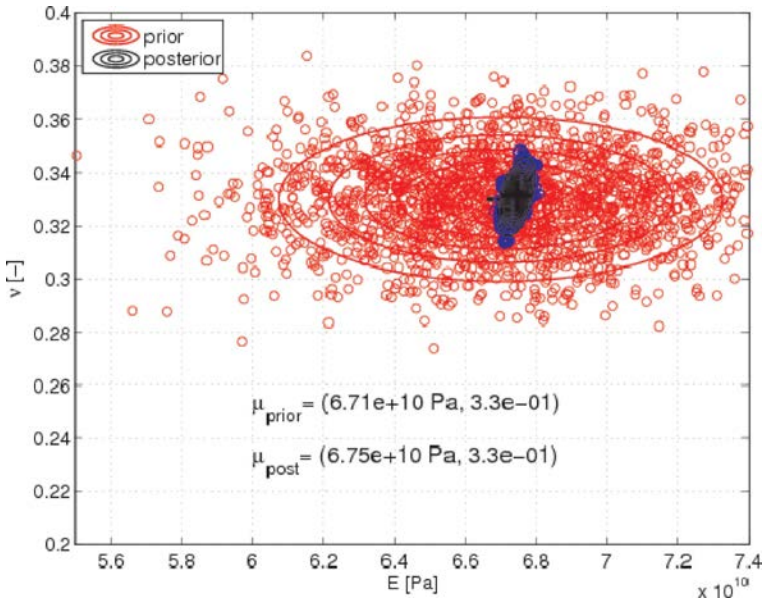

Fig. 7. Contour and scatter plots of prior and posterior distributions for Young's modulus and Poisson's ratio.

scatter plot of particles sampled from that prior. Table 3 presents statistical parameters of the prior.

Table 3. Statistical parameters of the Gaussian prior distribution for Young's modulus and Poisson's ratio.

Parameter	E [GPa]	ν
Mean value	67.1	0.330
Standard deviation	3.40	0.017
COV (%)	5.1	5.1

4.2.2. Results

As in the first example, the approximate posterior distribution of elastic constants given pseudo-experimental dispersion curves $P_N(\mathbf{x}_k|\mathbf{y}_k)$ in the k-th step was computed using the particle filter-based identification procedure described above. In the second experiment, we applied $N = 2000$ particles to approximate the posterior distribution and the number of steps was $K = 500$.

Figure 7 shows the contour plot of the posterior distribution together with the scatter plot of particles. Table 4 presents final identification results of elastic constants in the form of statistical parameters. From Tables 1 and 4, it can be concluded that the mean values of the posterior distribution are the same as the assumed elastic constants. Moreover, from Tables 3 and 4 it can be stated that in case of Young's modulus the coefficient of variation decreased from 5.1% for the prior distribution to only 0.3% for the posterior distribution. In case of Poisson's ratio the coefficient

Table 4. Statistical parameters of the posterior distribution for Young's modulus and Poisson's ratio.

Parameter	E [GPa]	ν
Mean value	67.5	0.33
Standard deviation	0.22	0.01
COV (%)	0.3	2

of variation decreased from 5.1% for the prior distribution to 2.0% for the posterior distribution which indicates that the identified Poisson's ratio is more uncertain.

5. Final remarks

The purpose of this paper was to present a novel application of particle filter for reconstruction of elastic constants of plate structures. The proposed procedure rests on the comparison of experimental and numerical dispersion curves in the context of Bayesian state estimation.

Taking into account the assumed experimental errors and considering propagation of errors in the sequential estimation, the uncertainty in the identified value of Poisson's ratio is 2% and the uncertainty in the estimated value of Young's modulus is less than 0.5%.

Acknowledgements

The financial support of the Polish National Science Centre Grant no. 2011/01/B/ST8/07210 "Theoretical basis for structural health monitoring by means of inverse problem solution under uncertainty" is gratefully acknowledged. Author is also very grateful to Prof. T. Uhl, supervisor of the Grant and Prof. Z. Waszczyszyn for their fruitful remarks. Author would like also to acknowledge the support from F.A. Amirkulova by sharing the Matlab scripts in her Master Thesis.

References

[1] F.A. Amirkulova. *Dispersion relations for elastic waves in plates and rods*. Master's Thesis, Rutgers, The State University of New Jersey, 2011.

[2] T. Furukawa, J.W. Pan. Stochastic identification of elastic constants for anisotropic materials. *International Journal for Numerical Methods in Engineering*, **81**(4): 429–452, 2010.

[3] C. Gogu, W. Yin, R. Haftka, P. Ifju, J. Molimard, R. Le Riche, A. Vautrin. Bayesian identification of elastic constants in multi-directional laminate from Moiré interferometry displacement fields. *Experimental Mechanics*, 635–648, 2013.

[4] H. Lamb. On waves in an elastic plate. *Proceedings of the Royal Society of London. Series A*, **93**(648): 114–128, 1917.

[5] W.P. Rogers. Elastic property measurement using Rayleigh-Lamb waves. *Research in Nondestructive Evaluation*, **6**(4): 185–208, 1995.

[6] J.L. Rose. *Ultrasonic waves in solid media*. Cambridge University Press (New York), 1999.

[7] S. Russel, P. Norvig. *Artificial intelligence: a modern approach*. Prentice Hall, 3rd Ed., 2010.

[8] M. Sale, P. Rizzo, A. Marzani. Semi-analytical formulation for the guided waves-based reconstruction of elastic moduli. *Mechanical Systems and Signal Processing*, **25**(6): 2241–2256, 2011.

[9] M. Tekieli, M. Słoński. Application of Monte Carlo filter for computer vision-based Bayesian updating of finite element model. *Mechanics and Control*, **33**(1): 2014.